Journal of Coordination Chemistry

ISSN: 0095-8972 (Print) 1029-0389 (Online) Journal homepage: http://www.tandfonline.com/loi/gcoo20

Synthesis, spectral characterization and crystal structure studies of a new hydrazone Schiff base and its dioxomolybdenum(VI) complex

Reza Kia & Hadi Kargar

To cite this article: Reza Kia & Hadi Kargar (2015) Synthesis, spectral characterization and crystal structure studies of a new hydrazone Schiff base and its dioxomolybdenum(VI) complex, Journal of Coordination Chemistry, 68:8, 1441-1451, DOI: 10.1080/00958972.2015.1011146

To link to this article: http://dx.doi.org/10.1080/00958972.2015.1011146

Journal of Coordination Chemistry, 2015
Vol. 68, No. 8, 1441–1451, http://dx.doi.org/10.1080/00958972.2015.1011146

Synthesis, spectral characterization and crystal structure studies of a new hydrazone Schiff base and its dioxomolybdenum(VI) complex

REZA KIA*† and HADI KARGAR*‡

†Chemistry Department, Sharif University of Technology, Tehran, Iran
‡Department of Chemistry, Payame Noor University, Tehran, Iran

(*Received 6 July 2014; accepted 20 November 2014*)

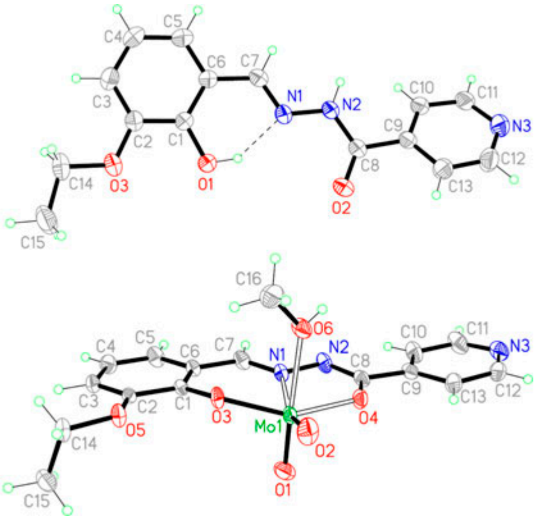

A new hydrazone-Schiff base (H_2L) and it corresponding dioxomolybdenum(VI) complex were synthesized and characterized by spectroscopic methods and elemental analyses. The crystal structures of both ligand and its complex were determined by single-crystal X-ray diffraction.

A new hydrazone Schiff base, (*E*)-*N*′-(3-ethoxy-2-hydroxybenzylidene)isonicotinohydrazide (H_2L), has been prepared and characterized by elemental analyses, spectroscopic methods, and single-crystal X-ray diffraction. The corresponding dioxomolybdenum(VI) complex $[Mo(O)_2(L)(CH_3OH)]$ was synthesized and characterized by spectroscopic methods and by single-crystal X-ray diffraction. The hydrazone ligand coordinates to Mo through the phenolate O, imine N, and enolic O. The Mo center displays a distorted octahedral geometry with the three donors of the ligands and an oxo defining the equatorial plane, and one methanol and another oxo occupying the axial positions.

Keywords: Hydrazone Schiff base; Molybdenum(VI) complexes; Crystal structure; Metal-oxo

---

*Corresponding authors. Email: rkia@sharif.edu; zsrkk@yahoo.com (R. Kia); h.kargar@pnu.ac.ir (H. Kargar)

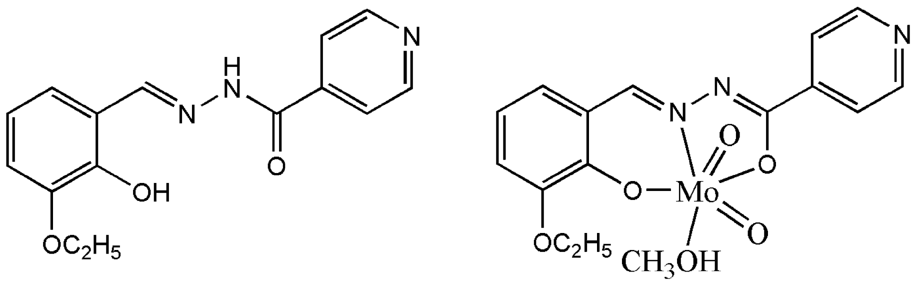

Figure 1. The chemical scheme of the hydrazone-Schiff base ligand (H_2L) and its Mo(VI) complex.

1. Introduction

The coordination chemistry of molybdenum(VI) has attracted interest for biochemical significance [1–3] and as catalysts in industrial processes such as epoxidation of olefins [4–8], olefin metathesis [9], isomerization of allylic alcohols [10], and oxidation of sulfides [11, 12]. Dioxomolybdenum(VI) complexes have been studied as models for the oxidized forms of molybdoenzymes, such as aldehyde oxidase and sulfite oxidase which are supposed to have $Mo(X)_2$ units (X = O, S) coordinated to sulfur, nitrogen, and oxygen donors of the protein structure [13, 14]. Schiff bases are among the most used ligands in coordination chemistry [15]. They owe their popularity to the frequent occurrence of C=N bonds in natural systems, as well as the fact that varying derivatives are comparatively easy to synthesize, providing ligands of different structures. A large number of dioxomolybdenum(VI) complexes of tetradentate Schiff base ligands with the $Mo(O)_2$ fragment have been studied [16–23], but for Mo(VI) complexes of isonicotinohydrazone Schiff bases [24–29], the number of crystal structures are rather few [30]. Here, we report the synthesis, spectroscopic characterization, and crystal structure of a new hydrazone Schiff base, (*E*)-*N*′-(3-ethoxy-2-hydroxybenzylidene)isonicotinohydrazide (H_2L). The corresponding dioxomolybdenum(VI) complex $[Mo(O)_2(L)(CH_3OH)]$ was also synthesized and characterized by spectroscopic methods and X-ray crystallography (figure 1).

2. Experimental

2.1. *Materials and methods*

Ammonium molybdate, acetylacetone (acac), 3-ethoxysalicylaldehyde, and isonicotinohydrazide were purchased from Aldrich. $[Mo(O)_2(acac)_2]$ was prepared and purified as described previously [31]. All other reagents were used as received. NMR spectra were recorded at ambient temperature with BRUKER AVANCE 500 MHz spectrometer using DMSO-d_6 as solvent. The chemical shift values (δ) are given in ppm. The infrared spectra (4000–400 cm^{-1}) were recorded in KBr disks with an IR Prestige-21 Shimadzu FT-IR spectrophotometer. Microanalyses (CHN) of the ligand and the complex were carried out on a Leco CHNS elemental analyzer.

2.2. *Synthesis of H_2L^1*

A hot methanol solution (25 mL) of 3-ethoxysalicylaldehyde (1.66 g, 10 mM) and isonicotinohydrazide (1.37 g, 10 mM) in 25 mL methanol were stirred under reflux for 1 h and cooled to room temperature. The precipitate was then filtered, washed with methanol, and dried *in vacuo*. Suitable single crystals for X-ray diffraction were obtained from hot methanol solution. Yield: 93%, m.p. 178–180 °C. ^{1}H NMR (500 MHz, DMSO-d_6, 25 °C): $\delta = 12.27$ (s, 1 H, –OH), 10.72 (s, 1 H, –NH), 8.69 (s, 1 H, –CHN), 8.78 [d, ^3J(H,H) = 5.55 Hz, 2 H, H (11,12)], 7.85 [d, ^3J(H,H) = 5.95 Hz, 2 H, H (10,13)], 7.17 [dd, ^3J(H,H) = 7.75 Hz, ^4J(H,H) = 0.95 Hz, 1 H, H (5)], 7.00 [dd, ^3J(H,H) = 7.90 Hz, ^4J(H,H) = 0.85 Hz, 1 H, H (3)], 6.82 [d, ^3J(H,H) = 7.90 Hz, 1 H, H (4)], 4.04 [q, ^3J(H,H) = 6.95 Hz, 2 H, –OCH_2], 1.33 [t, ^3J(H,H) = 6.95 Hz, 3 H, –CH_3] ppm. ^{13}C NMR (500 MHz) $\delta = 161.2$, 150.3, 149.1, 147.5, 147.1, 139.9, 121.4, 120.7, 119.1, 118.9, 115.4, 84.1, 14.7 ppm. IR (KBr, cm^{-1}); 3200 ($\nu_{N\text{–}H}$); 1693 ($\nu_{C=O}$); 1602 ($\nu_{C=N}$); 1564, 1466, ($\nu_{C=C}$); 1257 ($\nu_{C\text{–}O}$); 1041 ($\nu_{N\text{–}N}$). Anal. Calcd for $C_{15}H_{15}N_3O_3$ (285.3) (%): C, 63.15; H, 5.30; N, 14.73. Found (%): C, 63.17; H, 5.23; N, 14.85.

2.3. *Synthesis of $[Mo(O)_2(L)(CH_3OH)]$*

To a stirred solution of H_2L^1 (0.285 g, 1 mM) in 50 mL methanol was added $MoO_2(acac)_2$ (0.33 g, 1 mM). The resulting mixture was refluxed for 1 h. The orange reaction solution was filtered and the solvent removed under reduced pressure, yielding the complex as a red solid. Red single crystals suitable for X-ray diffraction were obtained by recrystallization of the solid from methanol. Yield: 87%, m.p. (decomposed) 290–291 °C. ^{1}H NMR (500 MHz,

Table 1. Crystal data and refinement parameters for H_2L and $[Mo(O)_2L(MeOH)]$.

Empirical formula	$C_{15}H_{15}N_3O_3$	$C_{16}H_{17}N_3O_6Mo$
Formula weight	285.30	443.27
Temperature (K)	291(2)	291(2)
Crystal system	Monoclinic	Monoclinic
Space group	$P2_1/n$	$P2_1/a$
a (Å)	7.4413(14)	12.107(5)
b (Å)	10.5454(10)	8.178(5)
c (Å)	17.958(3)	17.945(5)
α (°)	90	90.000(5)
β (°)	93.317(13)	99.615(5)
γ (°)	90	90.000(5)
Volume (Å^3)	1406.8(4)	1751.8(14)
Z	4	4
ρ_{calc} (mg mm^{-3})	1.347	1.681
μ (mm^{-1})	0.096	0.787
$F(0\ 0\ 0)$	600	896
Crystal size (mm)	0.08 × 0.11 × 0.21	0.07 × 0.15 × 0.19
Θ range for data collection	2.2°–50°	2.3°–29°
Index ranges	$-7 \le h \le 8$, $-12 \le k \le 11$, $-21 \le l \le 21$	$-16 \le h \le 16$, $-11 \le k \le 9$, $-24 \le l \le 23$
Reflections collected	6619	11,446
Independent reflections, R(int)	2429 (0.03)	4630 (0.06)
Data/restraints/parameters	2429/0/191	4630/0/237
Goodness-of-fit on F^2	0.988	1.036
Final R indexes [$I > 2\sigma(I)$]	$R_1 = 0.0407$, $wR_2 = 0.0956$	$R_1 = 0.0651$, $wR_2 = 0.0739$
Final R indexes (all data)	$R_1 = 0.0637$, $wR_2 = 0.1037$	$R_1 = 0.1234$, $wR_2 = 0.0840$
Largest peak/deepest hole (e Å^{-3})	−0.17/0.13	−0.71/0.65

DMSO-d$_6$, 25 °C): $\delta = 8.99$ (s, 1 H, iminic H), 8.75 [br, 2 H, H (11,12)], 7.86 [d, ^3J(H,H) = 9.46 Hz, 2 H, H (10,13)], 7.33 [d, ^3J(H,H) = 13.10 Hz, 1 H, H (5)], 7.26 [dd, ^3J(H,H) = 13.30 Hz, ^4J(H,H) = 1.80 Hz, 1 H, H (3)], 7.02 [d, ^3J(H,H) = 13.20 Hz, 1 H, H (4)], 4.12 [q, ^3J(H,H) = 8.75 Hz, 1 H, -OH (methanol)], 4.04 [q, ^3J(H,H) = 11.55 Hz, 2 H, $-OCH_2$], 3.15 [d, ^3J(H,H) = 8.75 Hz, 3 H, $-CH_3$ (methanol)], 1.33 [t, ^3J(H,H) = 11.55 Hz, 3 H, $-CH_3$] ppm. IR (KBr, cm^{-1}); 3333 (ν_{O-H}) (coordinated methanol); 1599 ($\nu_{C=N}$); 1523 ($\nu_{C=N-N=C}$); 1562, 1444, ($\nu_{C=C}$); 1246, 1157 (ν_{C-O}); 1041 (ν_{N-N}); 935 ($\nu_{O=Mo=O}$) *asym*; 910 ($\nu_{O=Mo=O}$) *sym*; 600 (ν_{Mo-O}); 470 (ν_{Mo-N}). Anal. Calcd (%) for $C_{16}H_{17}MoN_3O_6$: C, 43.35; H, 3.87; N, 9.48. Found (%): C, 43.48; H, 3.81; N, 9.32.

2.4. *Crystal structure determination*

Single-crystal X-ray data for H_2L and $[Mo(O)_2(L)(CH_3OH)]$ were collected at 296(2) K on a STOE IPDS 2T diffractometer with Mo Kα radiation ($\lambda = 0.71073$ Å). The unit cell parameter refinement, data reduction, and correction for Lp and decay were performed using X-AREA [32] software. Absorption corrections were applied using MULABS [33] routine in PLATON [34]. The structures were solved by direct methods and refined by least squares on F^2 using the SHELXTL program package [35]. All calculations were done by PLATON. All non-hydrogen atoms were refined anisotropically. The C-bound hydrogens were positioned geometrically and refined with a riding model approximation with their parameters constrained to the parent atom with U_{iso} (H) = 1.2 or 1.5 U_{eq} (C). The O-bound hydrogens in the ligand and complexes were located from the difference Fourier map and constrained to refine with the parent atoms with U_{iso} (H) = 1.5 U_{eq} (O). The crystal data and refinement parameters of H_2L and its complex are shown in table 1. Selected bond lengths and angles of H_2L and its complex are listed in table 2. The hydrogen bonding data are summarized in table 3.

Table 2. The selected bond lengths (Å) and angles (°) in H_2L and $[Mo(O)_2L(MeOH)]$.

Ligand			
C(7)–N(1)	1.271(2)	O(1)–C(1)–C(6)	122.50(14)
C(1)–O(1)	1.354(2)	C(1)–C(6)–C(7)	121.43(14)
N(1)–N(2)	1.375(2)	C(6)–C(7)–N(1)	121.55(13)
N(2)–C(8)	1.353(2)	C(7)–N(1)–N(2)	117.89(12)
C(8)–O(2)	1.212(2)	N(1)–N(2)–C(8)	118.23(11)
C(1)–C(6)	1.399(2)	N(2)–C(8)–O(2)	123.91(14)
Complex			
Mo(1)–O(1)	1.684(4)	O(1)–Mo(1)–O(2)	105.94(17)
Mo(1)–O(2)	1.697(3)	O(1)–Mo(1)–O(3)	99.90(14)
Mo(1)–O(3)	1.923(3)	O(1)–Mo(1)–O(4)	95.12(14)
Mo(1)–O(4)	2.027(3)	O(1)–Mo(1)–O(6)	167.24(13)
Mo(1)–O(6)	2.316(3)	O(1)–Mo(1)–N(1)	91.53(15)
Mo(1)–N(1)	2.239(4)	O(2)–Mo(1)–N(1)	160.95(15)
N(1)–C(7)	1.277(6)	O(2)–Mo(1)–O(4)	98.77(14)
N(1)–N(2)	1.408(5)	O(2)–Mo(1)–O(3)	101.74(13)
C(8)–O(4)	1.309(5)	O(2)–Mo(1)–O(6)	85.62(14)
C(1)–O(3)	1.354(5)	O(3)–Mo(1)–O(4)	150.07(10)

Table 3. Hydrogen bonding parameter in H_2L and $[Mo(O)_2L(MeOH)]$.

	D−H···A	D−H	H···A (Å)	D···A (Å)	D−H···A (°)
Ligand	O(1)–H(1)···N(1)	0.87	1.85	2.6124(16)	145
	N(2)–H(2)···N(3)[a]	0.87	2.26	3.1309(18)	175
Complex	O(6)–H(6)···N(3)[b]	0.85	1.91	2.723(5)	162
	C(5)–H(5A)···O(1)[c]	0.93	2.49	3.114(6)	124

Symmetry codes:
[a] $3/2 - x$, $1/2 + y$, $1/2 - z$.
[b] $-x$, $-y$, $1 - z$.
[c] $-1/2 + x$, $3/2 - y$, z.

3. Results and discussion

The hydrazone Schiff base (H_2L) was readily synthesized by condensation of 3-ethoxysalicyaldehyde with isonicotinhydrazide in methanol, followed by recrystallization from methanol. The dioxomolybdenum(VI) complex of the synthesized ligand was prepared by reaction of $Mo(O)_2(acac)_2$ with H_2L in methanol. H_2L adopts an enolic tautomeric form upon complexation. The ligand and its molybdenum complex are stable in air for an extended period of time and are soluble in DMF, DMSO, chloroform, dichloromethane, and acetonitrile.

3.1. *NMR spectra*

Typical ^1H NMR spectra of the ligand and its corresponding complex recorded at room temperature are shown in supplementary material (figures S1 and S2, see online supplemental material at http://dx.doi.org/10.1080/00958972.2015.1011146). The $^{13}C\{^1H\}$ NMR spectrum of H_2L with details of the peak assignment is shown in supplementary material (figure S3). In the ^1H NMR spectrum of the ligand a signal at δ 12.27 ppm is assignable to –OH, while a signal at δ 10.72 ppm is assigned to –NH. The spectrum of the complex clearly shows the disappearance of –OH and –NH signals of the ligand in the complex, indicating the site of coordination with the metal ion. This shows that keto-imine tautomerism has occurred upon complexation. Furthermore, a singlet at δ 8.69 ppm (azomethine proton) in the spectrum for the ligand showed downfield shift by 0.3 ppm to δ 8.99 ppm upon complexation. This is due to the reduction of electron density of the azomethine linkage as a result of coordination of nitrogen, resulting in the deshielding of the azomethine proton. This is in agreement with the IR spectrum of the complex, in which ν(C=N) is smaller than that in the ligand. This observation indicates that the C=N nitrogen is the third coordinating site. Aromatic protons of the ligand and complex appear within the expected range. A quartet at δ 4.04 ppm [^3J (H,H) = 6.95 Hz] is assigned to the $-OCH_2$ protons, coupled with the $-CH_3$ protons, while a triplet at δ 1.33 ppm [^3J (H,H) = 6.95 Hz] is assigned to the $-CH_3$ protons, coupled with the $-OCH_2$ protons. The range of chemical shifts observed for aliphatic protons did not show any appreciable change upon complexation. The spectrum of the complex also showed a doublet at δ 3.15 ppm [^3J (H,H) = 8.75 Hz] assigned to $-CH_3$ protons and quartet at δ 4.12 ppm [^3J (H,H) = 8.75 Hz] assigned to the –OH proton of coordinated methanol.

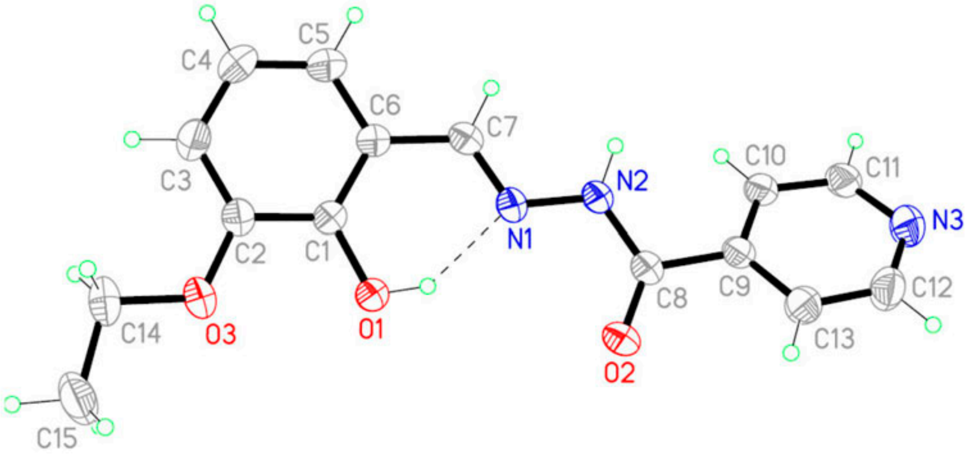

Figure 2. The molecular structure of H_2L with displacement ellipsoids at 40% probability and atom numbering scheme.

3.2. *IR spectra*

IR spectra of H_2L and its dioxomolybdenum(VI) complex are shown in supplementary material (figures S4 and S5). The bonding sites of the ligand involved in coordination with the metal ion have been further examined by careful comparison of IR spectra of the free ligand and its complex. The IR spectrum of the free ligand exhibit two bands at 3200 and 1693 cm^{-1} due to v(NH) and v(C=O). The absence of these bands in the spectrum of the complex is consistent with enolization of the amide functionality and subsequent proton replacement by the metal ion [27]. This type of coordination mode has been confirmed by X-ray analysis of the complex. Weak coordination of methanol *trans* to the oxo group is not uncommon in dioxomolybdenum complexes with tridentate ligands when the complexes are synthesized or crystallized in methanol [27, 29]. A new band at 1257 cm^{-1} is assigned

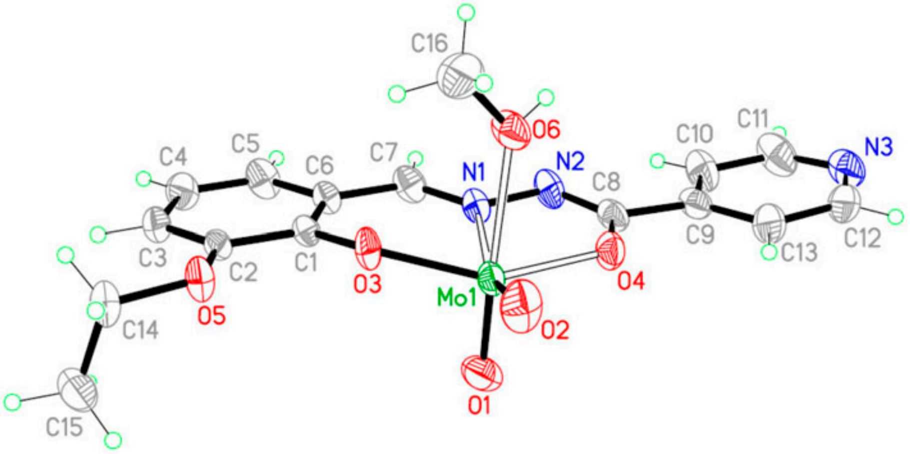

Figure 3. The molecular structure of the complex with displacement ellipsoids at 50% probability and atom numbering scheme.

to the *v*(C–O) (enolic) mode. Unequivocal assignment of the *v*(C=N) (azomethine) as well as *v*(C=C) (ring) stretches of the ligand could not be carried out due to the complexity of the spectrum in the 1600 $\mathrm{cm^{-1}}$ region. The band due to *v*(N–N) appears at 995 $\mathrm{cm^{-1}}$ in the free ligand. On coordination this band shifts from 46 $\mathrm{cm^{-1}}$ to higher wavenumbers and falls within the range commonly observed for monodentate coordination of the >N–N< residue.

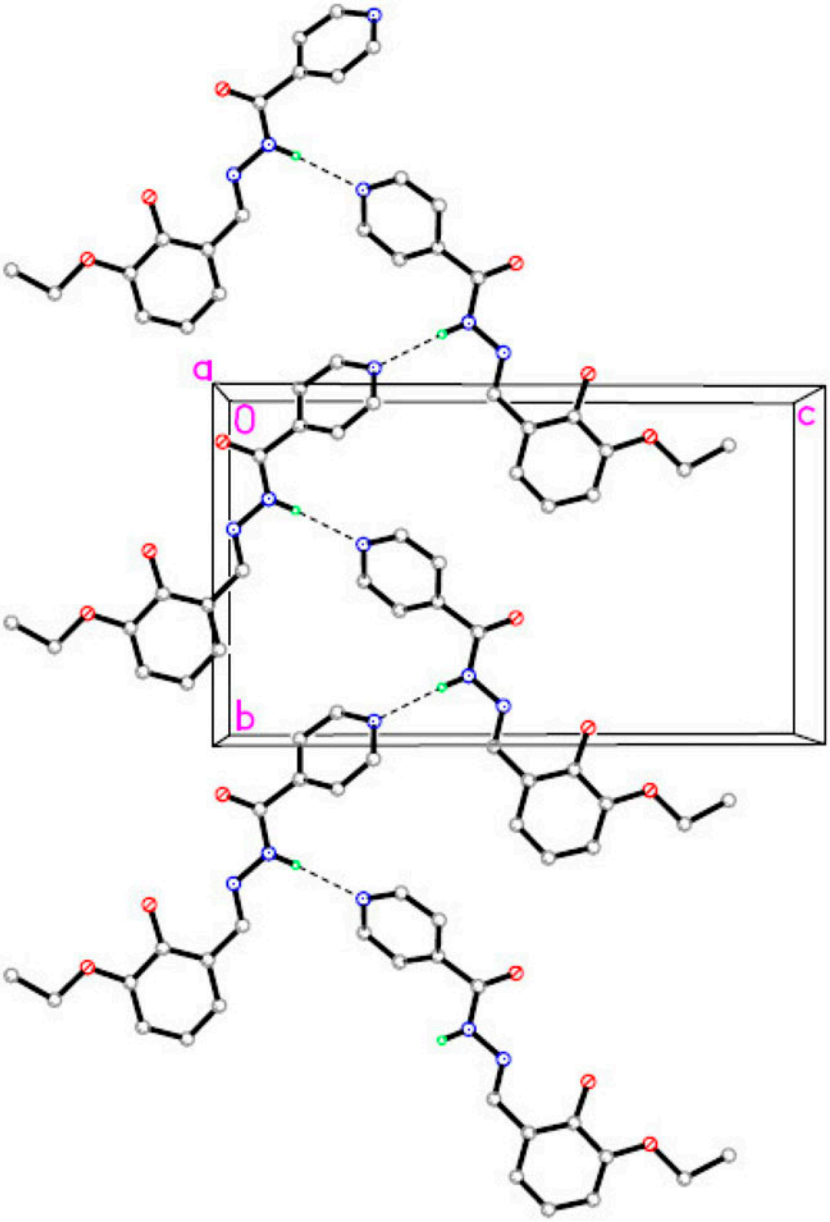

Figure 4. The packing of H_2L viewed down the *a*-axis showing *zigzag* linking of the molecules by the intermolecular N–H···N hydrogen bonds.

The high frequency shift is expected because of the diminished repulsion between lone pairs of adjacent nitrogens. The two prominent bands at 935 and 910 cm^{-1} attributed to the symmetric and asymmetric stretch of *cis*-$Mo(O)_2$ are consistent with previously reported complexes [25]. Bands indicative of Mo–O and Mo–N vibrations are at 600 and 470 cm^{-1}, respectively, and are also in agreement with those observed in similar complexes [36]. A band at 3450 cm^{-1} may be attributed to coordinated methanol.

3.3. *Description of the crystal structures*

The molecular structures of H_2L and the dioxomolybdenum(VI) complex are shown in figures 2 and 3, respectively. The crystal packing of H_2L and the Mo complex are shown in figures 4–6. The hydrazone Schiff base (H_2L) crystallizes in the monoclinic system with space group $P2_1/n$. The hydrogen of the hydroxyl group shows a strong intramolecular O–H···N hydrogen bond. The substituted benzene ring is not coplanar with the pyridine ring, as the dihedral angle is 31.39(9)°. The bond lengths and angles in H_2L are comparable to those observed in similar hydrazone Schiff bases [37–39].

In the crystal packing of H_2L, the molecules are linked by intermolecular N–H···N hydrogen bonds, forming a *zig-zag* array along the *b*-axis (figure 4). The complex crystallizes in the monoclinic system with space group $P2_1/a$. In the complex, the coordination geometry around molybdenum can be described as distorted octahedral in which two *cis* positions are occupied by two oxo groups, in agreement with the IR spectroscopic data, a dianionic tridentate hydrazone Schiff base ligand and a methanol molecule. The distortion of the octahedral coordination of the structure can also be understood from the bond angles around Mo, which are summarized in table 2. Upon coordination the dihedral angle between the substituted benzene ring and pyridine [3.9(2)°] in the complex significantly decreases compared to the free ligand [31.39(9)°]. The Mo is displaced by 0.299(1) Å from the best equatorial coordination plane of N1/O2/O3/O4. These donors deviate by ±0.0021 Å from the best least-squares plane. The Mo–O and Mo–N bond lengths in the complex are comparable to those observed in previously reported dioxomolybdenum(VI) complexes with hydrazone

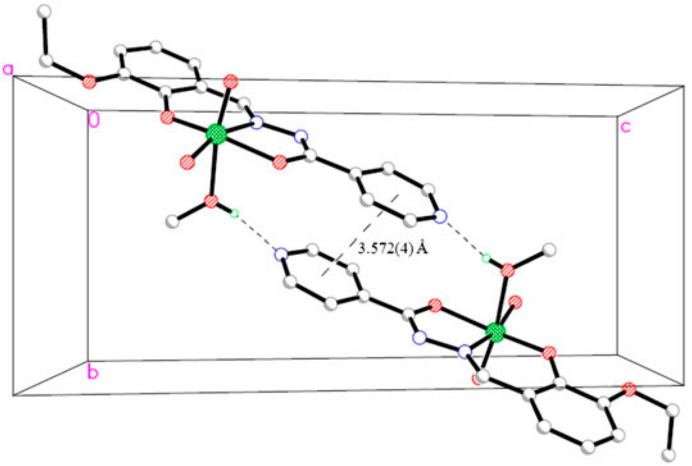

Figure 5. Part of packing of the complex, showing individual dimer formation by centrosymmeric O–H···N hydrogen bonds supported by π–π interaction.

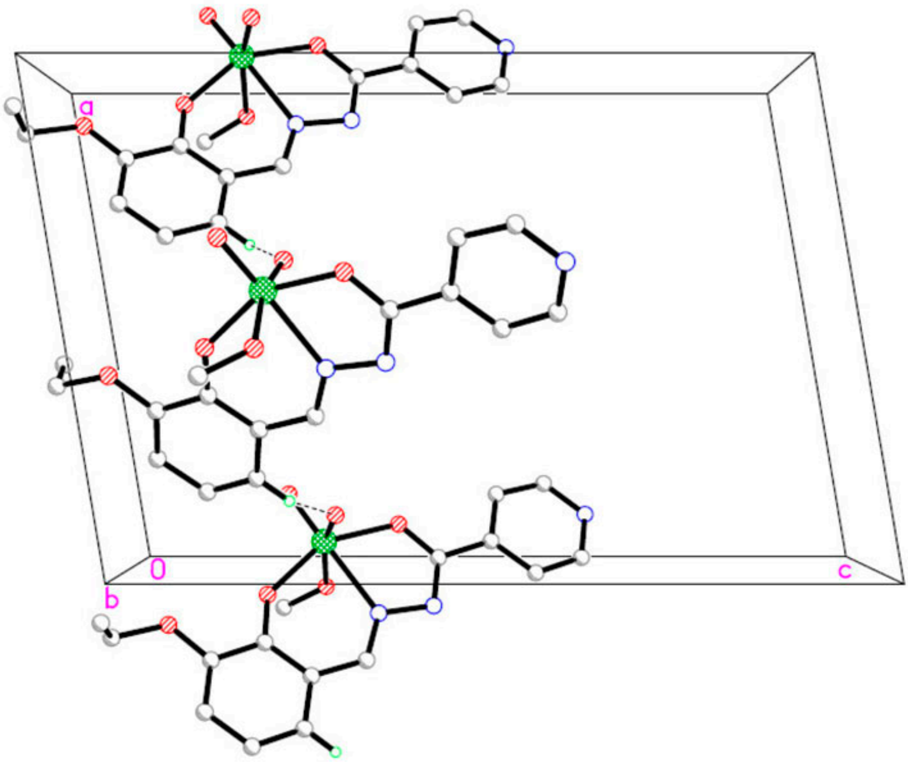

Figure 6. The packing of the complex viewed down the *b*-axis showing a 1-D extended chain of molecules connected by the intermolecular C–H···O interactions along the *a*-axis.

ligands [40–46]. The bond lengths of the N1–N2 [1.408(5) Å] and iminic N1–C7 [1.277(6) Å] groups were increased upon coordination to the molybdenum center in agreement to previously reported structures [42–46]. As observed in similar complexes, the elongated Mo1–O6 [2.316(3) Å] bond length *trans* to oxo O1 group indicates weak coordination of methanol at the axial position. This is due to the strong π-donor character of the oxo *trans* to coordinated methanol [41–46]. The two Mo=O bond distances and the subtended O(1)=Mo(1)=O(2) are comparable to previously reported molybdenum complexes [40–46]. In the crystal packing of the complex, centrosymmetric O–H···N hydrogen bonds form individual dimers, in which the mutual pyridine rings show $\pi \cdots \pi$ interaction with a centroid to centroid distance of 3.572(4) Å (figure 5). The crystal packing is further stabilized by intermolecular C–H···O interactions, which link neighboring molecules into a 1-D extended chain along the *a*-axis (figure 6).

4. Conclusion

A new tridentate hydrazone Schiff base ligand was synthesized by condensation of 3-ethoxysalicyaldehyde with isonicotinhydrazide in refluxing methanol and characterized by elemental analyses, spectroscopic methods, and X-ray diffraction analysis. Using the synthesized hydrazone ligand, a new dioxomolybdenum(VI) complex was prepared and fully characterized by spectroscopic methods and X-ray crystallography. Similar to other reported dioxomolybdenum(VI) complexes, the mode of coordination of the hydrazone ligand is tridentate through phenolate O, imino N, and enolate O from the enol-tautomeric form of the ligand along with the typical *cis* arrangement of the two terminal oxo groups.

Supplementary material

Crystallographic data for the structural analysis have been deposited with the Cambridge Crystallographic Data Center as supplementary publication Nos. CCDC 1010204 and 1010205 for the ligand and its complex, respectively. Copies of this information may be obtained free of charge via http://www.ccdc.cam.ac.uk/conts/retrieving.html or from the Director, CCDC, 12 Union Road, Cambridge, CB2 1EZ, UK (Fax: +44 1223 336 033; E mail: deposit@ccdc.ac.uk).

Acknowledgments

RK thanks Sharif University of Technology Research council for the facility. HK is grateful to Payame Noor University of Ardakan for providing the research facilities.

References

[1] D. Collison, C.D. Garner, J.A. Joule. *Chem. Soc. Rev.*, **25**, 25 (1996).
[2] R. Hille. *Chem. Rev.*, **96**, 2757 (1996).
[3] G.C. Tucci, J.P. Donahue, R.H. Holm. *Inorg. Chem.*, **37**, 1602 (1998).
[4] B.E. Schultz, S.F. Gheller, M.C. Muetterties, M.J. Scott, R.H. Holm. *J. Am. Chem. Soc.*, **115**, 2714 (1993).
[5] M. Bagherzadeh, M. Zare, V. Amani, A. Ellern, L.K. Woo. *Polyhedron*, **53**, 223 (2013).
[6] M. Bagherzadeh, R. Latifi, L. Tahsini, V. Amani, A. Ellern, L.K. Woo. *Polyhedron*, **28**, 2517 (2009).
[7] M. Bagherzadeh, L. Tahsini, R. Latifi, L.K. Woo. *Inorg. Chim. Acta*, **362**, 3698 (2009).
[8] S. Rayati, N. Rafiee, A. Wojtczak. *Inorg. Chim. Acta*, **386**, 27 (2012).
[9] R.K. Grasselli. *Catal. Today*, **49**, 141 (1999).
[10] R.J. Cross, P.D. Newman, R.D. Peacock, D. Stirling. *J. Mol. Catal.*, **144**, 273 (1999).
[11] M. Bagherzadeh, M.M. Haghdoost, A. Ghanbarpour, M. Amini, H.R. Khavasi, E. Payab, A. Ellern, L.K. Woo. *Inorg. Chim. Acta*, **411**, 61 (2014).
[12] M. Bagherzadeh, L. Tahsini, R. Latifi, A. Ellern, L.K. Woo. *Inorg. Chim. Acta*, **361**, 2019 (2008).
[13] K.J. Ivin, J.C. Mol. *Olefin Metathesis and Metathesis Polymerization*, Academic Press, London (1997).
[14] J. Belgacem, J. Kress, J.A. Osborn. *J. Am. Chem. Soc.*, **114**, 1501 (1992).
[15] P.J. Brower. *Transition Met. Chem.*, **23**, 109 (1998).
[16] K. Yamanouchi, S. Yamada. *Inorg. Chim. Acta*, **9**, 161 (1974).
[17] W.E. Hill, N. Atabay, C.A. McAuliffe, F.P. McCullough, S.M. Razzoki. *Inorg. Chim. Acta*, **35**, 35 (1979).
[18] M. Gullotti, A. Pasini, G.M. Zanderighi, G. Ciani, A. Sironi. *J. Chem. Soc., Dalton Trans.*, 902 (1981).
[19] H. Elias, F. Stock, C. Röhr. *Acta Crystallogr.*, **C53**, 862 (1997).
[20] C. Sun, X.-Y. Wang, Z.-G. Zhang, H.-C. Shi. *Chin. J. Org. Chem.*, **24**, 547 (2004).
[21] W. Schilf, B. Kamieński, Z. Rozwadowski, K. Ambroziak, B. Bieg, T. Dziembowska. *J. Mol. Struct.*, **700**, 61 (2004).
[22] K. Ambroziak, R. Pelech, E. Milchert, T. Dziembowska, Z. Rozwadowski. *J. Mol. Catal. A: Chem.*, **211**, 9 (2004).
[23] X. Zhou, J. Zhao, A.M. Santos, F.E. Kuhn. *Z. Naturforsch*, **59b**, 1223 (2004).
[24] Y. Lei, C. Fu. *Synth. React. Inorg. Met.-Org., Nano-Met. Chem.*, **41**, 704 (2011).
[25] V. Vrdoljak, B. Prugovečki, D.M. Calogovic, J. Pisk, R. Dreos, P. Siega. *Cryst. Growth Des.*, **11**, 1244 (2011).
[26] S.K. Kurapati, U. Ugandhar, S. Maloth, S. Pal. *Polyhedron*, **42**, 161 (2012).
[27] S.-P. Gao. *J. Coord. Chem.*, **64**, 2869 (2011).

[28] W.-X. Xu, Y.-M. Yuan, W.-H. Li. *J. Coord. Chem.*, **66**, 2726 (2013).
[29] Y.-M. Cui, Y. Wang, Y.-J. Cai, X.-J. Long, W. Chen. *J. Coord. Chem.*, **66**, 2325 (2013).
[30] F.H.Allen.*Acta Crystallogr., Sect. B: Struct. Sci.*, **58**, 380 (2002); *ConQuest (Version 1.16)* (2014).
[31] G.J.-J. Chen, J.W. McDonald, W.E. Newton. *Inorg. Chem.*, **15**, 2612 (1976).
[32] Stoe & Cie. *X-AREA*, Stoe & Cie, Darmstadt (2009).
[33] R.H. Blessing. *Acta Crystallogr., Sect. A: Found. Crystallogr.*, **51**, 33 (1995).
[34] A.L. Spek. *Acta Cryst.*, **D65**, 148 (2009).
[35] G.M. Sheldrick, SHELXTL (Version 5.1), Bruker Analytical X-ray Instruments Inc., Madison, WI, USA (1998).
[36] M. Bagherzadeh, M. Amini, H. Parastar, M. Jalali-Heravi, A. Ellern, L.K. Woo. *Inorg. Chem. Commun.*, **20**, 86 (2012).
[37] Z.-P. Li, Y.-J. Li, Z.-X. Li, H. Li, Z.-P. Xiao. *J. Chem. Crystallogr.*, **41**, 1568 (2011).
[38] G. Dutkiewicz, B. Narayana, S. Samshuddin, H.S. Yathirajan, M. Kubicki. *J. Chem. Crystallogr.*, **41**, 1442 (2011).
[39] H. Kargar, R. Kia, M. Akkurt, O. Büyükgüngör. *Acta Crystallogr.*, **E66**, 2982 (2010).
[40] A. Rana, R. Dinda, P. Sengupta, S. Ghosh, L.R. Falvello. *Polyhedron*, **21**, 1023 (2002).
[41] S. Gao, X.-F. Zhang, L.-H. Huo, H. Zhao. *Acta Crystallogr.*, **E60**, m1731 (2004).
[42] V. Vrdoljak, M. Cindrić, D. Milić, D. Matković-Čalogović, P. Novak, B. Kamenar. *Polyhedron*, **24**, 1717 (2005).
[43] S.-B. Ding, W.-H. Li. *J. Coord. Chem.*, **66**, 2023 (2013).
[44] N.-Y. Jin. *J. Coord. Chem.*, **65**, 4013 (2012).
[45] X.-Q. He. *J. Coord. Chem.*, **66**, 966 (2013).
[46] A.-M. Li. *J. Coord. Chem.*, **67**, 1022 (2014).